

Collision avoidance in low thrust rendezvous guidance using flatness and positive B-splines

Christophe Louembet, Georgia Deaconu

Abstract— Collision avoidance issue in close proximity orbital rendezvous is addressed in this paper. The arising optimal control problem is solved by means of differential flatness in order to apply algebraic geometry tools. These tools based on B-splines parametrization and positive piecewise polynomial concept provide a certification of constraints satisfaction continuously in time contrary to classical collocation techniques. The non convexity derived from the avoidance constraint is overcome by using time-varying convex approximation.

I. INTRODUCTION

Spacecraft rendezvous is an enabling technology for present and future space missions.

In recent years, electric propulsion has been used and proposed for many space applications including orbit transfers and station keeping (see [2], [1], [11]), but also for interplanetary and deep space missions (see [20], [10]). A direct method is exploited here, for the ease of handling linear and non linear path constraints on contrary to the Pontryagin's maximum principle methods. These methods, based on parametrization and/or discretization of the original optimal control problem (see [12]) have been successful in solving both impulsive and continuous thrust rendezvous problem under path constraints (see for instance [4] for impulsive maneuver and [3] for electric propulsion and the references therein).

In this paper, the focus is on the collision avoidance issue in close proximity maneuvers. This issue has been studied from different points of view, for both impulsive and continuous thrust. A popular approach in path planning community is the artificial potential technique which consists in completing the dynamics of the flying formation with a force derived from a potential such that the two spacecraft are repelled from each others, [13]. Another strategy to ensure a safety distances between spacecrafts is to add to the cost function a penalty term, [3]. These two approaches can be related to the electrostatic collision avoidance technique developed by [24] where the spacecraft are charged with positive or negative electric potential and take advantage of the derived Coulomb force.

In the same time, collision avoidance can be addressed by adding avoidance constraints to the parametric optimisation problem and applying the pertinent programming solver. Thus, early works from [6] consisted in solving the avoidance constraints with a non linear programming solver. Unfortunately, from the non convexity of the avoidance

problem follows the existence of multiple local minima. [21] addressed this drawback in the framework of linear Hill-Chloehessy-Wiltshire relative motion model by enforcing a rectangular exclusion region around vehicles and using the mixed integer linear programming. Finally, in order to obtain a convex program, the exclusion region constraints have been replaced by a rotating convex approximation in [19], [4]. The late papers are interesting since they imply convex linear programs that are known to be computationnally tractable. The proposed methodology is based on differential flatness (see [8]) and aims to ensure constraints satisfaction all along the path on the contrary to classical direct methods as developed in [19], [4].

Using differential flatness, eligible optimal control problems could be solved by means of geometric techniques (and thus avoiding integration of the dynamics) using the flat trajectory parametrization. In the differential flatness context, a classical and tractable methodology developed in [18], [7], [17] relies on B-splines based collocation. However, as in classical direct methods, this technique involves time sampling: constraints satisfaction between collocation points can not be guaranteed. This may lead to critical issues that need to be detected by an appropriate post-analysis (see examples from [4], [17] for instance). In this paper, our goal is to design flat system trajectories, using the convenient B-splines parametrization, that guarantees continuous constraints satisfaction in time using positive piecewise polynomials concept and, thus, avoids the need for post-analysis .

In section II, we briefly present the relative motion model and the concept of differential flatness. Then, the optimal path planning problem for flat systems is described. Our contribution is detailed in section III in two steps. First, in subsection III-A, the results on positive polynomials from [16] is presented. Subsequently, in subsection III-B, the constrained B-splines optimization is formulated as a convex optimization problem over linear matrix inequalities (LMI) for which efficient programming (SDP) solvers are available. In section IV, an example of the resolution of an orbital homing problem illustrates the methodology.

II. PROBLEM STATEMENT

A. Relative motion model

In this paper, the Rendezvous mission consists of two spacecraft: a chaser satellite with full 3-axis capability and a passive target spacecraft on an arbitrary elliptic orbit. This particular relative motion between the two satellites in close space was firstly described in [23]. In the following, we

Christophe Louembet and Georgia Deaconu are with LAAS-CNRS; Université de Toulouse ; 7 avenue du colonel Roche, F-31077 Toulouse, France louembet@laas.fr

describe briefly the development of the equations of motions in order to obtain a state model of the relative dynamics. In the context of an elliptic keplerian orbit, the linearized relative motion is stated by the so-called Tshauer-Hempel equations:

$$\begin{cases} \ddot{x} = 2n \frac{(1+e \cos \nu)^2}{(1-e^2)^{3/2}} \dot{y} - 2n^2 e \sin \nu \left(\frac{1+e \cos \nu}{1-e^2} \right)^3 y \dots \\ \quad + n^2 \left(\frac{1+e \cos \nu}{1-e^2} \right)^3 (3 + e \cos \nu) x + n^2 u_R \\ \ddot{y} = -2n \frac{(1+e \cos \nu)^2}{(1-e^2)^{3/2}} \dot{x} + 2n^2 e \sin \nu \left(\frac{1+e \cos \nu}{1-e^2} \right)^3 x \\ \quad + n^2 \left(\frac{1+e \cos \nu}{1-e^2} \right)^3 (e \cos \nu) y + n^2 u_S \\ \ddot{z} = -n^2 \left(\frac{1+e \cos \nu}{1-e^2} \right)^3 z + n^2 u_W \end{cases} \quad (1)$$

where ν is the true anomaly, e is the eccentricity, n is the mean motion and the input vector $u(t)$ is derived from the propulsion force F_{chaser} and the m_{chaser} :

$$\begin{cases} u_R = \frac{F_{chaser,R}}{m_{chaser} n^2} \\ u_S = \frac{F_{chaser,S}}{m_{chaser} n^2} \\ u_W = \frac{F_{chaser,W}}{m_{chaser} n^2} \end{cases} \quad (2)$$

Simplified Tschauner-Hempel equations can be obtained by replacing time as the independent variable with the true anomaly, ν , and by using a classical change of variables (see [23] for detail):

$$\begin{cases} \tilde{x}'' = 2\tilde{y}' + \frac{3}{1+e \cos \nu} \tilde{x} + \tilde{u}_R \\ \tilde{y}'' = -2\tilde{x}' + \tilde{u}_S \\ \tilde{z}'' = -\tilde{z} + \tilde{u}_W \end{cases} \quad (3)$$

We can now define the state vector $\tilde{X}(\nu) = [\tilde{x} \ \tilde{y} \ \tilde{z} \ \tilde{x}' \ \tilde{y}' \ \tilde{z}']$ and the associated input vector $\tilde{u} = [\tilde{u}_R \ \tilde{u}_S \ \tilde{u}_W]$ and deduce the linear time-periodic state space model:

$$\frac{d\tilde{X}(\nu)}{d\nu} = \tilde{A}_{TH} \tilde{X}(\nu) + \tilde{B}_{TH} \tilde{u}(\nu) \quad (4)$$

with:

$$\tilde{A}_{TH} = \begin{bmatrix} 0 & 0 & 0 & 1 & 0 & 0 \\ 0 & 0 & 0 & 0 & 1 & 0 \\ 0 & 0 & 0 & 0 & 0 & 1 \\ \frac{3}{1+e \cos \nu} & 0 & 0 & 0 & 2 & 0 \\ 0 & 0 & 0 & -2 & 0 & 0 \\ 0 & 0 & -1 & 0 & 0 & 0 \end{bmatrix} \quad \tilde{B}_{TH} = \begin{bmatrix} 0 & 0 & 0 \\ 0 & 0 & 0 \\ 0 & 0 & 0 \\ 1 & 0 & 0 \\ 0 & 1 & 0 \\ 0 & 0 & 1 \end{bmatrix} \quad (5)$$

B. Differential flatness

Differential flatness, or flatness in short, has been introduced [8] in 1992. Consider a nonlinear system:

$$\dot{X} = f(X, u), \quad (6)$$

where X is the n -component state vector and u the m -component control vector, $m \leq n$.

Definition 1: The nonlinear system (6) is differentially flat if there exists an m -dimensional vector χ , whose elements are differentially independent, such that:

$$\chi = \Phi(X, u, \dot{u}, \dots, u^{(\alpha)}), \quad (7)$$

and:

$$\begin{cases} X = \Psi_X(\chi, \dot{\chi}, \dots, \chi^{(\beta-1)}), \\ u = \Psi_u(\chi, \dot{\chi}, \dots, \chi^{(\beta)}), \end{cases} \quad (8)$$

where Ψ_X and Ψ_u are smooth functions, $\chi_i^{(k)}$ denoting the k^{th} order time derivative of the i^{th} component of χ , and the multi-index $\beta = (\beta_1, \dots, \beta_m)$ contains the characteristic numbers associated to the flat outputs and is defined by:

$$\beta_i = \min \left\{ k \in \mathbb{N}^* : \partial \left(\frac{d^k \chi_i}{dt^k} \right) / \partial u_j \neq 0, j \in \{1, \dots, m\} \right\} \quad (9)$$

with $i = 1, \dots, m$. The elements of $\chi \in \mathbb{R}^m$ are called flat outputs.

Since we focus our attention on linear systems, we recall from [9] the following result:

Proposition 1: A linear system is flat if and only if it is controllable

In our case, system (4) is fully controllable since the chaser is fully actuated. One can easily check that the controllability matrix of the pair $(\tilde{A}_{TH}, \tilde{B}_{TH})$ is full-row rank for $e < 1$. Consequently, system (4) is differentially flat. Moreover, an eligible flat output is the position vector $\chi = [\tilde{x} \ \tilde{y} \ \tilde{z}]^T$ (see [14, footnote 2] for complementary explanations). Thus function Ψ is trivial and function Ψ_u is obtained by inverting Tshauer Hempel equations (3):

$$\begin{cases} \tilde{u}_R = \chi_1'' - \frac{3}{1+e \cos \nu} \chi_1 - 2\chi_2' \\ \tilde{u}_S = \chi_2'' + 2\chi_1' \\ \tilde{u}_W = \chi_3'' + \chi_3 \end{cases} \quad (10)$$

The real interest of flatness for optimal control problem is that it also defines a Lie-Bäcklund equivalence between a nonlinear system and a trivial system (see [9] for explanations). As χ represent the state of the trivial system, the m -components of χ are differentially independent. Indeed, a $\bar{\chi}$ -space of dimension n_χ can be considered with the coordinates $\bar{\chi} = \{\chi, \chi', \chi'', \dots, \chi^{(p)}\}$ with $p \in \mathbb{N}$ where any curve in this space is equivalent to the system trajectories.

As it will be described in the next paragraph, the solution to the optimal control problem can be described as a particular curve of the $\bar{\chi}$ -space.

C. Flat formulation of the RdV guidance problem

Generating a constrained trajectory consists in determining a finite-time trajectory $t \mapsto (\tilde{X}(\nu), \tilde{u}(\nu))$ with $\nu \in [\nu_i; \nu_f]$, satisfying the set of constraints related to the dynamics of the underlying system, boundary conditions, path and actuators constraints. The problem can be formulated as follows:

$$\begin{aligned} \min_{\tilde{u}} J(\tilde{X}, \tilde{u}) \quad \text{subject to:} \quad & \begin{cases} \frac{d\tilde{X}(\nu)}{d\nu} = \tilde{A}_{TH} \tilde{X}(\nu) + \tilde{B}_{TH} \tilde{u}(\nu), \\ \tilde{X}(\nu_i) = \tilde{X}_0, \quad \tilde{u}(\nu_i) = \tilde{u}_0, \\ \tilde{X}(\nu_f) = \tilde{X}_f, \quad \tilde{u}(\nu_f) = \tilde{u}_f, \\ \gamma(\tilde{X}(\nu), \tilde{u}(\nu)) \geq 0, \end{cases} \end{aligned} \quad (11)$$

where $J(\tilde{X}, \tilde{u})$ represents a particular objective function and $\gamma(\tilde{X}(\nu), \tilde{u}(\nu))$ the path and actuators constraints. The path

and actuators constraints are such that:

$$-\tilde{U}_{max} \leq \tilde{U}_i \leq \tilde{u}_{max}, \quad i = \{R, S, W\} \quad (12)$$

$$\tilde{x}^2 + \tilde{y}^2 \geq d^2 \quad (13)$$

Constraint (12) comes from the saturation on the actuators. Indeed, from equation (10), the saturation constraints may be expressed in terms of $\bar{\chi}$:

$$\begin{cases} -\tilde{U}_{max} \leq \chi_1'' - \frac{3}{1+e \cos \nu} \chi_1 - 2\chi_2' \leq \tilde{U}_{max} \\ -\tilde{U}_{max} \leq \chi_2'' + 2\chi_1' \leq \tilde{U}_{max} \\ -\tilde{U}_{max} \leq \chi_3'' + \chi_3 \leq \tilde{U}_{max} \end{cases} \quad (14)$$

Alternatively, the saturation constraint can be defined as the membership of the trajectory $\bar{\chi}(t)$ to a polytope of $O_{\bar{\chi}}$ described by its cartesian coordinates:

$$H_{sat}(\nu)\bar{\chi}(\nu) \leq \tilde{U}_{max}. \quad (15)$$

In order to have a constant matrix H , the variant term $\frac{3}{1+e \cos \nu}$ is replaced by its worst case approximation: upper and lower bound $\frac{3}{1+e}$ and $\frac{3}{1-e}$ such that:

$$H_{sat} = \begin{bmatrix} \frac{3}{1-e} & 0 & -1 & 0 & 2 & 0 & 0 & 0 & 0 \\ -\frac{3}{1+e} & 0 & 1 & 0 & -2 & 0 & 0 & 0 & 0 \\ 0 & -2 & 0 & 0 & 0 & -1 & 0 & 0 & 0 \\ 0 & 2 & 0 & 0 & 0 & 1 & 0 & 0 & 0 \\ 0 & 0 & 0 & 0 & 0 & 0 & -1 & 0 & -1 \\ 0 & 0 & 0 & 0 & 0 & 0 & 1 & 0 & 1 \end{bmatrix} \quad (16)$$

Equation (13) represents the collision avoidance constraint. The definition of the collision avoidance is that trajectory can not cross the cylindric safe zone around the target. A such constraint is given by $\tilde{x}^2 + \tilde{y}^2 \geq d^2$ that is non linear and non convex. As in [19], the late collision avoidance definition is replaced by the fact that the position must lie in a halfspace defined by a tangent line to the circle with the general equation $\tilde{x} \cos \beta + \tilde{y} \sin \beta = d$.

The collision avoidance constraint will then be derived as

$$-\chi_1 \cos \beta - \chi_2 \sin \beta \leq -d \quad (17)$$

In order to drive round the safe region, we will enforce the rotation of the half plane defining the feasible region. In order to achieve this, the angle $\beta(\nu)$ is a piecewise constant function. The consequence is that the constraint (17) remains linear in χ and is constant piecewisely during the maneuver time.

Using the specific flatness properties, the optimal control problem (11) is transformed into the following problem:

Problem 1: Considering the flat system (6), the optimal path planning problem (11) can be formulated as the following optimization problem:

$$\min_{\bar{\chi}} J(\bar{\chi}(\nu)) \quad \begin{cases} \bar{\chi}(\nu_i) = \bar{\chi}_i, \\ \bar{\chi}(\nu_f) = \bar{\chi}_f, \\ \bar{\chi}(\nu) \in S_{\bar{\chi}}, \end{cases} \quad (18)$$

where $\bar{\chi}$ are flat space coordinates, $J(\bar{\chi})$ is assumed to be convex in terms of $\bar{\chi}$ and the subset $S_{\bar{\chi}}$, the so-called feasible region, is defined by equations (15) and (17). Note that, since

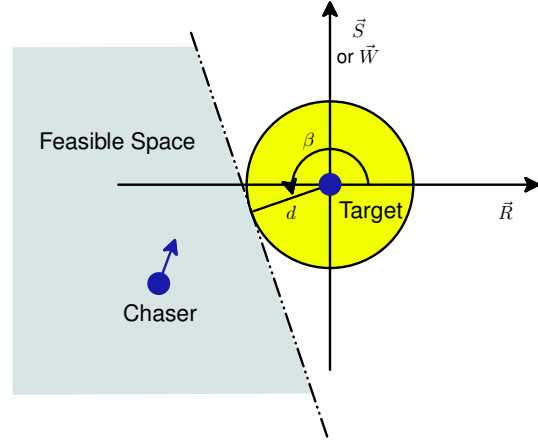


Fig. 1. Convex approximation of the non convex avoidance region

only the second derivative of χ is involved in system (14), we will consider the $\bar{\chi}$ -space $O_{\bar{\chi}}$ such that:

$$O_{\bar{\chi}} = \{\chi, \chi', \chi''\} \quad (19)$$

The dimension of $O_{\bar{\chi}}$ is 9.

D. B-splines Parametrization

Then, by virtue of (18), it turns out that the optimal control problem for a flat system consists in determining a finite time trajectory $\nu \mapsto \chi(\nu)$ that connects two points of the $\bar{\chi}$ -space and belongs to the subset $S_{\bar{\chi}}$. Since all curves of $\bar{\chi}$ -space verify the nonlinear system dynamics, problem (11) is equivalent to the geometric and integration-free problem (18). One of the advantages of problem 1 is that it can be solved by all algorithms able to determine curves belonging to a well-determined subspace. The B-splines formalism from [18], [17], [17] offers a convenient framework to define piecewise polynomial trajectories and constraints (particularily piecewise constant constraints) providing high flexibility with a low number of parameters. Indeed, in this paper, the trajectories of the flat output χ components and their derivatives are represented with a B-splines basis:

$$\begin{aligned} \chi_i(\nu) &= \sum_{j=1}^{n_B} C_{i,j} \cdot B_{j,k}(\nu), & i = 1, \dots, m \\ \chi_i^{(r)}(\nu) &= \sum_{j=1}^{n_B} C_{i,j} \cdot B_{j,k}^{(r)}(\nu), & i = 1, \dots, m. \end{aligned} \quad (20)$$

Here $\{B_{j,k}\}$ is a k^{th} order B-splines basis built on a given knot sequence T (see [17] for further details on B-splines usage and [5, chap. VIII] for complete definitions). The control points $C_{i,j}$ are the coordinates of the piecewise polynomials $\chi_i(\nu)$ in the B-splines basis. Let C be the vector of the control points defining the trajectories $\chi(\nu)$:

$$C = (C_{1,1}, \dots, C_{1,n_B}, C_{2,1}, \dots, C_{2,n_B}, C_{3,1}, \dots, C_{3,n_B}) \in \mathbb{R}^{N_C}$$

Using a B-splines parameterization of the flat output, the control points C become the decision variables of the flat optimal control problem (18).

Problem 2: Consider flat system (6), the optimal path planning problem using B-splines parametrization can be formulated as follows:

$$\min_C J(\bar{\chi}(C)) \quad \begin{cases} \bar{\chi}(t_i, C) = \bar{\chi}_i, \\ \bar{\chi}(t_f, C) = \bar{\chi}_f, \\ \bar{\chi}(C) \in S_{\bar{\chi}}. \end{cases} \quad (21)$$

The constraint $\bar{\chi}(C) \in S_{\bar{\chi}}$ can be seen as an inclusion of $\bar{\chi}(\nu)$ trajectories within the intersection of several half-spaces. In fact, it will be shown that positioning the trajectory $\bar{\chi}(\nu)$ in a half-space is equivalent to evaluate the sign of the piecewise polynomial gap function, $\kappa(\nu)$, between $\bar{\chi}(\nu)$ and the hyper-plane boundary. Thus, this positioning problem is equivalent to a positivity problem of piecewise polynomials. By using the concept of positive B-splines developed through LMI approach in [16], the problem 2 will be recast as a semidefinite program providing solutions, if they exist, that verify the constraint $\bar{\chi}(C) \in S_{\bar{\chi}}$ all along the path.

III. PATH PLANNING AS A B-SPLINES POSITIVITY PROBLEM

A. Elements of piecewise polynomial positivity

In [16], the sums of squares representation of piecewise polynomials function has been developed. This representation is convenient since it permits to link the semidefinite positiveness of piecewise polynomial with the cone of semidefinite positive matrix. In fact, this set of positive piecewise polynomial is shown to be a linear image of the cone of the positive semidefinite matrices.

Let $P(t)$ be a piecewise polynomial defined on the B-splines basis $\{v_i(t)\}$ such that $P(t) = \sum_{i=1}^{n_v} \mu_i v_i(t)$ with μ being the coordinates of $P(t)$ on $v_i(t)$. Through the linear operator Λ^* , the set of the coefficients μ may be described on a B-spline basis $v(t)$ that define a positive piecewise polynomial function.

Theorem 1: Let μ be an element of the closed, pointed and convex cone K defined by:

$$K = \{\mu \in \mathbb{R}^{n_v} : \mu = \Lambda^*(Y), Y \succeq 0\}. \quad (22)$$

Each element μ of K describes a positive semidefinite polynomial on the basis $v(t)$ so that

$$P(t) = \sum_{i=1}^{n_v} \mu_i v_i(t) \geq 0. \quad (23)$$

In the aim of not duplicate information available in open literature, definitions of Λ^* and proof of the theorem 1 are detailed in [16].

B. Motion planning as an LMI problem

This result, mainly based on theorem 1, is the description of the piecewise polynomial trajectory inclusion into a polytope as a B-spline positivity problem and consequently as an LMI problem.

Let $O_{\bar{\chi}}$ be the finite dimensional flat output space with the following coordinates:

$$\bar{\chi} = (\chi_1, \dots, \chi_m, \dot{\chi}_1, \dots, \dot{\chi}_m, \chi_1^{(r)}, \dots, \chi_m^{(r)})$$

Recall that the flat trajectories $[\nu_0, \nu_f] \rightarrow \mathbb{R}^{n_{\bar{\chi}}}$, $\nu \mapsto \chi(\nu)$ are parametrized on k -order B-splines basis $\{B_k\}$ (see equation (20)).

Let the feasible region $S_{\bar{\chi}}$ be an intersection of n_c half-spaces of $O_{\bar{\chi}}$ and H_i be the i^{th} half-space described by its Cartesian coordinates:

$$H_i = \{\bar{\chi} \in \mathbb{R}^{n_{\bar{\chi}}} \mid a_i^T \bar{\chi} \leq b_i\}, \quad (24)$$

where $a_i \in \mathbb{R}^{n_{\bar{\chi}}}$ and $b_i \in \mathbb{R}$ are possibly piecewise polynomials in time with $i = 1, \dots, n_c$. We note that $\bar{\chi}(\nu)$ belong to the half-space H_i if and only if:

$$a_i^T \bar{\chi}(\nu) \leq b_i \quad (25)$$

Theorem 2: Solving the path planning problem defined by (21), is equivalent to solving the following SDP problem:

$$\begin{aligned} & \min_C J(\bar{\chi}(C)) \\ \text{subject to: } & \begin{cases} \alpha_i C - b_i = \Lambda^*(Y_i) \\ Y_i \succeq 0 \\ \Theta C = \theta \end{cases}, \forall i = 1, \dots, n_c. \end{aligned} \quad (26)$$

with the objective function assumed to be linear in $\bar{\chi}$ and in the control points

$$C = (C_{1,1}, \dots, C_{1,n}, C_{2,1}, \dots, C_{2,n}, C_{3,1}, \dots, C_{3,n})$$

as well.

Λ^* is the dual operator defined in [16]. $\alpha_i \in \mathbb{R}^{n_v \times N_C}$ are linear matrix functions of a_i , with a_i and b_i associated to the i^{th} half-space H_i (cf. equation (24)). The equality constraint $\Theta C = \theta$ represents the initial and final conditions.

The complete proof is detailed in [16]. Nevertheless, an insight may be that each sum from (24) of weighted flatout trajectories and their derivatives is piecewise polynomial $\kappa_{i=1, \dots, n_c}(\nu) = \sum_{j=1}^{n_v} \kappa_{i,j} v_j(\nu)$ defined on B-splines basis $v(\nu)$ such that $\kappa_i(\nu) \geq 0$. Finally the κ coefficients are determined using theorem 1.

Note that to match semidefinite program definition, the cost of problem (26) has to be linear in C .

IV. ORBITAL HOMING EXAMPLE

In this section, we detail the rendezvous problem and propose a solution using the methodology presented in section III. The studied case is inspired by the ATV mission. The Keplerian parameters of the target orbit are given in table I. Inclinaison, Perigee argument and RAAN parameters are omitted since a keplerian orbit is considered.

The trajectory $t \mapsto \chi(\nu)$ is a 5th order piecewise polynomial function defined on the sequence of equidistant knots $\xi = \{\xi_1, \dots, \xi_{15}\}$. Indeed $\chi(\nu)$ admits $B(\nu)$ as B-splines basis such that the trajectory can handle non zero initial and final conditions at (ξ_1 and ξ_{15}) and has the highest continuity degree at interior breakpoints (ξ_2 to ξ_{14})

TABLE I
MISSION EXAMPLE

Excentricity e	0.0052
Initial homing anomaly ν_1	0
Final homing anomaly ν_f	$5rad$
Initial state $\tilde{X}_1, [m, m/s]$	$[0, 50, 0, 0, 0, 0]$
Final state $\tilde{X}_f, [m, m/s]$	$[0, -30, 0, 0, 0, 0]$
Chaser's mass	$500 kg$
Actuator saturation	$1 N$

i.e 4.

The number, n_c , of linear constraints in $\bar{\chi}$, is 7 : 6 for the saturation constraints (equation (15)) and 1 for the collision avoidance (equation (17)). In order to define Λ^* , we need to characterize the gap functions $\kappa_i(\nu)$. Since the higher derivation order involved in saturation constraints (14) is two, the $\kappa_{i=1\dots 6}(\nu)$ are fifth order piecewise polynomials of continuity class C^0 at initial and final knots $\{\xi_1, \xi_{15}\}$ and C^2 at the interior knots $\{\xi_2, \dots, \xi_{14}\}$.

The constraint (17) involves linearly only the flat outputs but has piecewise constant coefficient. In fact, in order to enforce the bypass of the safe region, the angle β in (17) is piecewise constant function of time such that:

$$\beta = \beta_1 + i \left(\frac{\beta_f - \beta_1}{7} \right), \text{ if } \nu \in [\xi_{2i+1}, \xi_{2i+3}], i = 0 \dots 6 \quad (27)$$

β_1 and β_f are the direction angle to initial and final position in the orbit plane:

$$\beta_1 = \arctan \left(\frac{\tilde{X}_{1,S}}{\tilde{X}_{1,R}} \right), \beta_f = \arctan \left(\frac{\tilde{X}_{f,S}}{\tilde{X}_{f,R}} \right) \quad (28)$$

Thus, the gap function $\kappa_7(\nu)$ is C^0 at the odd knots $\xi_1, \xi_3, \dots, \xi_{15}$ and C^4 at even knots $\xi_2, \xi_4, \dots, \xi_{14}$. The operators Λ_i^* and coefficient matrices α_i of problem (26) are then calculated using methodology developed in [16]. Problem (26) is solved using Yalmip from [15] and Sedumi 1.02 from [22].

The obtained trajectory is given in figure 1. Figure 2 shows that the in-plane trajectory respects clearly the avoidance constraints.

For comparison, we solve problem (21) by means of flatness and collocation methods described in [17], [18], [7]. Recall that the constraints are checked in a finite number of time called collocation points. The problem is solved with the quadratic solver MATLAB `quadprog` considering 25 collocation points that are equidistant in anomaly. Although an admissible solution for the collocation problem is quickly obtained, the trajectory violates the constraints between the collocation points: the avoidance constraints for $\beta = \frac{5\pi}{6}, \pi, \frac{7\pi}{6}$ are obviously transgressed and constraints for $\beta = \frac{8\pi}{6}, \pi, \frac{3\pi}{2}$ are also violated (see figure 3). Moreover, we can observe on figure 3 that our methodology can produce trajectories very close to the bounds without violating them. On the contrary, when collocation points get closed to the boundaries, the situation could lead to constraints violation.

Thrust profiles along R and S direction are presented on figure 4. Both thrust profiles are equivalent and not saturated and the cost objectives are less than 3% different. With the above collocation methods, an iterative process is needed to re-distribute the sequence or increase the number the collocation points. This is to be compared to the one-shot method exposed in this paper.

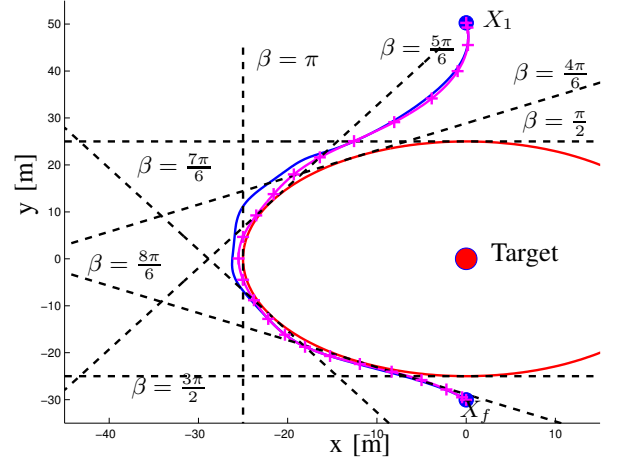


Fig. 2. Trajectories $\bar{\chi}(t)$ obtained by SDP (blue) and by collocation (magenta), the collocation points are the crosses point, red circle is the safe region, dash line are the sequential approximation of the safe zone

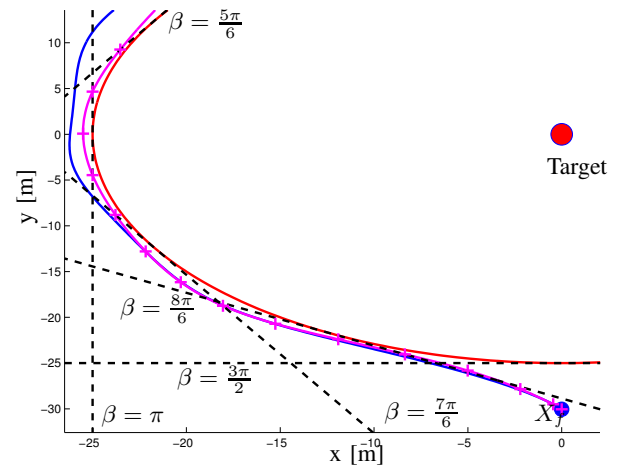


Fig. 3. Focus

V. CONCLUDING REMARKS

In this paper, the orbital rendezvous planning problem using continuous thrust is solved by means of a new approach based on the differential flatness and positive piecewise polynomials results. As opposed to most works on direct methods for optimal control problem reported in the literature, the developed methodology provides a new framework for satisfying constraints all along the path.

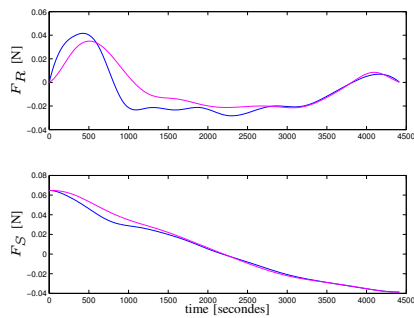


Fig. 4. Thrust profiles

REFERENCES

- [1] B. M. Anzel. Stationkeeping the hughes hs 702 satellite with a xenon ion propulsion system. In *49th International Astronautical Congress*, Melbourne, Australia, 1998.
- [2] B.M. Anzel. Controlling a stationary orbit using electric propulsion. In *DGLR/AIAA/ISASS 20th International Electric propulsion Conference*, Garmisch-Partenkirchen, Germany, 1988.
- [3] R. Armellin, M. Massari, and A.E. Finzi. Optimal Formation Flying Reconfiguration and Station Keeping Maneuvers Using Low Thrust Propulsion. In *18th International Symposium on Space Flight Dynamics*, volume 548, page 429. Munich, Germany: Oct, 2004.
- [4] L. Breger and J How. Safe trajectories for autonomous rendezvous of spacecraft. *Journal of Guidance, Control and Dynamics*, 31(5):1478–1489, 2008.
- [5] C. de Boor. A practical guide to spline. In *Applied Mathematical Sciences*, volume 27. Springer, 1978.
- [6] MC Eckstein, CK Rajasingh, and P. Blumer. Collocation strategy and collision avoidance for the geostationary satellites at 19 degrees west. In *International Symposium on Space Flight Dynamics*, volume 6, 1989.
- [7] N. Faiz, S.K. Agrawal, and R.M. Murray. Differentially flat systems with inequality constraints: An approach to real-time feasible trajectory generation. *J. Guidance, Control and Dynamics*, 24, 2001.
- [8] M. Fliess, J. Lévine, P. Martin, and P. Rouchon. On differentially flat nonlinear systems. *Proc. 2nd. IFAC NOLCOS Symposium Bordeaux*, 1992.
- [9] M. Fliess, J. Lévine, P. Martin, and P. Rouchon. a lie-bäcklund approach to equivalence and flatness of nonlinear systems. *IEEE Trans. Automat. Contr.*, 44(5):922–937, 1999.
- [10] J. Gil-Fernandez, E. Milic, M. Graziano, B. Polle, S. Mancuso, and J. Fertig. Autonomous low-thrust guidance scheme for interplanetary trajectories: Application to smart-1. In European Space Agency, editor, *6th International ESA Conference on Guidance, Navigation and Control Systems*, Loutraki, Greece, 17-20 October 2006.
- [11] N. S. Gopinath and K. N. Srinivasamuthy. Optimal low thrust orbit transfer from gto to geosynchronous orbit and stationkeeping using electric propulsion system. In *54th International Astronautical Congress of the International Astronautical Federation, the International Academy of Astronautics, and the International Institute of Space Law*, Bremen, Germany, 2003.
- [12] D. G. Hull. Conversion of optimal control problems into parameter optimization problems. *J. Guidance, Control and Dynamics*, 20(1), 1997.
- [13] O. Junge and S. Ober-Blobaum. Optimal reconfiguration of formation flying satellites. In *44th IEEE Conference on Decision and Control, 2005 and 2005 European Control Conference. CDC-ECC'05*, pages 66–71, 2005.
- [14] J. Lévine and D.V. Ngyuen. Flat output characterisation for linear systems using polynomial matrices. *Systems and Control Letters*, 48:69–75, 2003.
- [15] J. Löfberg. Yalmip : A toolbox for modeling and optimization in MATLAB. In *Proceedings of the CACSD Conference*, Taipei, Taiwan, 2004.
- [16] C. Louembet, F Cazaurang, and A Zolghadri. Motion planning for flat systems using B-splines parametrization:an LMI approach. *Automatica*, 46:1305–1309, 2010.
- [17] C. Louembet, F Cazaurang, A Zolghadri, C. Pittet, and C Charbonnel. Path planning for satellite slew maneuvers: A combined flatness and collocation based approach. *IET Control Theory & Applications*, 2009.
- [18] M.B. Milam, K. Mushambi, and R.M. Murray. A new computational approach to real-time trajectory generation for constrained mechanical systems. In *IEEE Conference on Decision and Control*, 2000.
- [19] J Mueller and R Larsson. Collision avoidance maneuver planning with robust optimization. In *7th International ESA Conference on Guidance, Navigation & Control Systems*, Tralee, County Kerry, Ireland, 2-5 June 2008.
- [20] M. Rayman, P. Chadbourne, J. Culwell, and S. William. Mission design for deep space 1: A low-thrust technology validation mission. *Acta Astronautica*, 45(4-9):381–388, August-November 1999.
- [21] A Richards, T Schouwenaars, J How, and E Feron. Spacecraft trajectory planning with avoidance constraints using mixed-integer linear programming. *Journal of Guidance, Control, and Dynamics*, 25(4):755–764, 2002.
- [22] J.F. Sturm. Using SEDUMI 1.02, a MATLAB toolbox for optimization over symmetric cones. *Optimization methods and software*, 11-12:625–653, 1999.
- [23] J. Tschauner. The elliptic orbit rendezvous. In *AIAA 4th Aerospace Sciences Meeting*, Los Angeles, California, USA, Juin 1966.
- [24] S. Wang and H. Schaub. Electrostatic Spacecraft Collision Avoidance Using Piecewise-Constant Charges. *Journal of guidance, control, and dynamics*, 33(2), 2010.